Pergamon

0042-6989(95)00182-4

Vision Res., Vol. 36, No. 8, pp. 1103–1114, 1996

Printed in Great Britain
0042-6989/96 $15.00 + .00

Off-axis Optical Quality and Retinal Sampling in the Human Eye

DAVID R. WILLIAMS,* PABLO ARTAL,† RAFAEL NAVARRO,‡ MATTHEW J. McMAHON,§ DAVID H. BRAINARD¶

Received 16 January 1995; in revised form 26 June 1995

Using the double pass procedure, Navarro *et al.* (1993; *Journal of the Optical Society of America A, 10*, 201–212) measured the monochromatic modulation transfer function (MTF) of the human eye as a function of retinal eccentricity. They chose conditions as similar as possible to those encountered in natural viewing. We report new measurements obtained with conditions chosen instead to optimize retinal image quality: we paralyzed accommodation, used a 3 mm pupil, and corrected defocus and oblique astigmatism at each retinal location. MTFs were estimated at the tangential focus, circle of least confusion, and sagittal focus produced by oblique astigmatism. Though optical blur is well-known to have little effect on peripheral visual acuity, it can nonetheless substantially reduce aliasing by receptoral and post-receptoral spatial sampling.

Aberrations Aliasing Oblique astigmatism Blur Peripheral vision

Several studies have measured the optical quality of the retinal image in peripheral retina (Jennings & Charman, 1978, 1981; Navarro *et al.*, 1993). Jennings and Charman (1978, 1981) measured the line spread function with the double pass technique (Flamant, 1955) and broad band illumination. They established that the optical quality of the eye declines slowly with retinal eccentricity, more slowly than the decline in visual performance attributable to the nervous system. Navarro *et al.* (1993), using an improved version of the double pass procedure (Santamaria *et al.* 1987), measured the two-dimensional monochromatic modulation transfer function with a point source imaged at various locations on the horizontal retinal meridian. Their results confirmed the conclusions of Jennings and Charman, and provided improved estimates of the off-axis modulation transfer function. They used natural pupils (4 mm diameter) and free accommodation. Binocular fixation was maintained on a target at a distance of 0.33 m and the point source used to assess image quality was kept at this same distance for all retinal eccentricities. The motivation behind their measurements was to estimate peripheral retinal image quality under normal viewing conditions. For this reason, off-axis refractive errors and oblique astigmatism, which generally grow with retinal eccentricity, were deliberately left uncorrected.

Though the study of Navarro *et al.* (1993) provides valuable measures of the optical quality that typically might be encountered in normal viewing, it is less useful in indicating what role the optics play in limiting visual performance under more optimal viewing conditions. Even in normal viewing, objects in peripheral vision can sometimes lie at distances at which they are in focus, despite a peripheral refractive error. Similarly, spatial frequency components at the right orientation and distance in peripheral retina could be immune to blurring by oblique astigmatism. Moreover, measurements of human visual performance in the laboratory often optimize retinal image quality, for example, by correcting defocus and oblique astigmatism and paralyzing accommodation. It would be valuable to have absolute measures of image quality under these conditions to assess the role of the optics on visual performance.

This paper extends the measurements of Navarro *et al.* (1993) by estimating the optimum retinal image quality at various retinal eccentricities when defocus alone has been corrected and when both defocus and astigmatism have been corrected. The general consensus has been that the optics play relatively little role in peripheral vision, with the limits set mainly by neural factors. Nonetheless, our measurements show that the optics make an important contribution to preventing aliasing in peripheral vision.

*To whom all correspondence should be addressed at Center for Visual Science, University of Rochester, Rochester, NY 14627, U.S.A.
†Laboratorio de Optica, Departamento de Fisica, Universidad de Murcia, Campus de Espinardo, 30071 Murcia, Spain.
‡Instituto de Optic, Consejo Superior de Investigaciones Científicas, Serrano 121, 28006 Madrid, Spain.
§Department of Psychology, University of California, San Diego, La Jolla, CA 92093, U.S.A.
¶Department of Psychology, University of California, Santa Barbara, Santa Barbara, CA 93106, U.S.A.

METHOD

Subjects

Measurements were made on the right eyes of two subjects, PA and DRW who were 32 and 40 years of age, respectively. Accommodation was paralyzed with 2 drops of cyclopentolate hydrochloride (1%).

Apparatus

The apparatus, shown in Fig. 1, is slightly modified from that used in earlier experiments and described in detail elsewhere (Williams *et al.*, 1994). An abbreviated description is provided here.

Illumination path

The source was a He–Ne laser (543 nm, 10 mW) chosen because wavelengths in the middle of the visible spectrum produce the best estimate of retinal image quality with the double-pass method (Westheimer & Campbell, 1962; Charman & Jennings, 1976; Williams *et al.*, 1994). The expanding beam from a point source, created by a spatial filter, was collimated by L_1 and passed through a 3 mm artificial pupil that was conjugate with the observer's natural pupil. This controlled pupil size while avoiding the complication of placing an artificial pupil in front of the cornea, out of the pupil plane. A pellicle reflected the beam into lens L_2 which lay one focal length from the artificial pupil. L_2 formed an image of the point source that the observer viewed through L_3, which lay one focal length from his pupil plane.

The subject's head was stabilized with a bite bar. For foveal measurements, subjects fixated the point source itself. For all extrafoveal measurements, observers fixated an LED viewed through a mirror and a lens, L_5, that focused it on the retina. The horizontal and vertical alignment of the pupil was established for each retinal eccentricity by centering the natural pupil with respect to the artificial pupil using images taken with a CCD camera. Since the plane of the natural pupil rotates with eye rotation, the artificial pupil in the illumination path was rotated so that it was always optically coplanar with the natural pupil, as shown in Fig. 1.

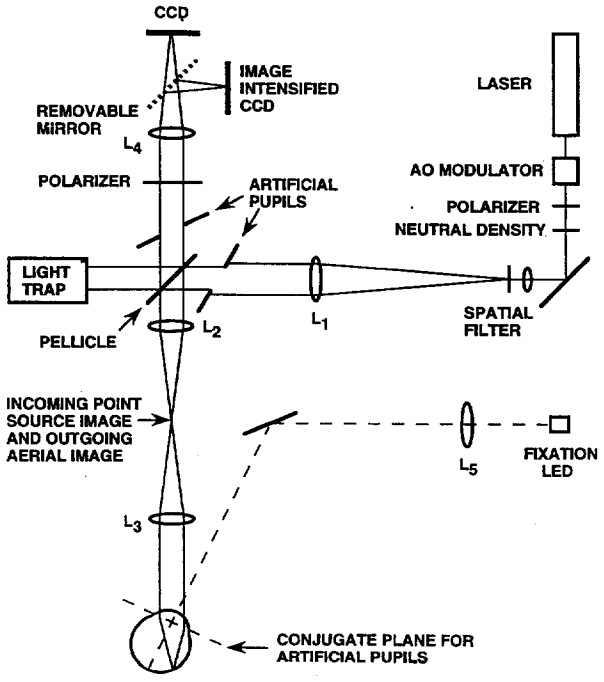

FIGURE 1. Double-pass apparatus (see text for details).

Light-collection path

Two vertically oriented linear polarizers, one in the illumination path and one in the light-collection path, reduced depolarized stray light in the system. The light reflected back out of the eye passed through a second artificial pupil which was registered optically with respect to the artificial pupil in the illumination path and was also 3 mm in diameter. For each retinal eccentricity, it was also rotated so that it was coplanar with the image of the plane of the natural pupil. This artificial pupil was one focal length from L_4. L_3 formed an aerial image of the point source one focal length from L_2. L_2 and L_4, which were separated by the sum of their focal lengths, re-imaged the aerial image on either of two CCD arrays discussed below.

Focusing

Before data collection began, the experimenter focused the point source on the observer's retina. This procedure also simultaneously focused the aerial image on the CCD array. A removable mirror was inserted beyond L_4 that directed the aerial image onto an image-intensified CCD. The video output of this CCD was displayed on a CRT. The experimenter then focused the point source by translating the subject's eye and lens L_3 together along the optical axis of the system. This technique, first employed by Arnulf *et al.* (1981) and used also by Williams *et al.* (1994), proved to be a particularly convenient and reliable way to identify the astigmatic foci along the Sturm interval.

At retinal eccentricities for which astigmatism was observed, aerial images were acquired in three different focusing conditions, corresponding to the tangential focus, the circle of least confusion, and the sagittal focus. In some cases, aerial images were also acquired with astigmatism corrected. This was achieved by bringing the sagittal focus into coincidence with the retina as described above and then adding a negative cylinder with its axis oriented approximately vertically and with a power corresponding to the Sturm interval. The appropriate axis for the trial lens was easily determined from the anisotropy in the aerial image displayed on the CRT. The trial lens was positioned at the spectacle point and perpendicular to the optical axis of the apparatus. For retinal eccentricities other than the fovea, the lens was therefore not perpendicular to the optical axis of the eye. This orientation was chosen to avoid the changes in trial lens power with oblique incidence.

Image acquisition

Once a particular focus was achieved with the image-intensified CCD, the mirror was removed and aerial images were acquired with the single frame CCD, which was the same distance from L_4. The single frame CCD has superior resolution and linearity making it more suitable for image acquisition, though it is too slow for focusing in real time. This CCD array was full frame and was cooled to reduce dark noise. Aerial images were 512 × 512 pixels with 12 bits/pixel. The magnification of the retinal image at the CCD was 7.2 times corresponding to a CCD field of view of 3.3 deg.

Aerial images were acquired at eccentricities of 0, 10, 20 and 40 deg in the temporal retina of each observer. The duration of each exposure was 5 sec. After an aerial image was acquired, a second image was acquired with the eye removed from the system. This second image was subtracted from the first to remove unwanted reflections and scatter from optical elements as well as bias charge on the CCD array. For each state of focus at each eccentricity, 10 such image pairs were collected and the difference images were averaged. A correction (flat fielding) was then applied to remove variations in intensity across the field caused by the apparatus and by nonuniformities in the CCD.

MTF computation

We computed the modulus of the Fourier transform of the processed, average aerial image. The square root of the modulus was taken as the single pass MTF. This MTF was corrected for the small amount of blurring produced by the CCD using the MTF for our CCD published by Marchywka and Socker (1992).

We also made a correction for the unwanted light in the aerial images from the Purkinje images. This light, which is almost entirely from the first surface of the cornea, arrives at the CCD as a relatively uniform background veil. It spuriously reduces the MTF at all non-zero spatial frequencies. MTFs corrupted by the corneal reflex have a characteristic, precipitous drop between zero and the first positive spatial frequencies, with an abruptly shallower slope thereafter. Williams *et al.* (1994) developed a method to correct the MTF with radiometric measurements of the Purkinje images. In the course of this work, they observed that MTFs that are either corrected for the Purkinje images, or were obtained in situations where the Purkinje images could not contribute, lack this abrupt drop near zero spatial frequency. Instead, they initially fall approximately linearly from a value of unity. We capitalized on this property to remove the corneal reflection. We removed all values of the MTF at spatial frequencies less than 1 c/deg and linearly extrapolated the missing values based on the data between 1 and 2 c/deg. To produce the final MTF, the MTF was normalized by dividing it by the extrapolated value at zero spatial frequency. This operation is essentially equivalent to subtracting from the aerial image a uniform background produced by the Purkinje images and is much less difficult than measuring the corneal reflection directly in order to remove it.

Contrast sensitivity measurements

We also report here some interferometric contrast sensitivity measurements in the peripheral retina made 8 years ago with an interferometer described by Williams (1985a). The wavelength was 632.8 nm, retinal illuminance was 500 td, and the diameter of the test field was 3.3 deg. Each trial consisted of two, 500 msec intervals marked by tones. One interval, randomly determined from trial to trial, contained an interference fringe and one contained a uniform field. The interference fringe presented on each trial was either horizontal or vertical, also randomly determined from trial to trial. The observer made two judgments on each trial: he guessed the fringe orientation and the interval in which it was presented. The fringe contrast was controlled in independent staircase procedures to provide two estimates of contrast sensitivity at each spatial frequency. The orientation judgment was used to estimate contrast sensitivity for resolving the stripes of the fringe, whereas the interval judgment was used to estimate contrast sensitivity for detecting the fringe at low frequencies or its alias at higher frequencies.

AERIAL IMAGE RESULTS

Figure 2 reviews the geometry and nomenclature of oblique astigmatism, which is typically the dominant monochromatic aberration in the periphery. When a point source is displayed along a retinal meridian from the optical axis of the eye, the power of the eye is greater for rays lying in that same meridian of the eye's optics than in the perpendicular meridian. This produces two distinct foci instead of one. At the tangential focus, the point spread function is narrowest in the direction parallel to the displacement of the point source from the optic axis and is elongated in the perpendicular direction. For the horizontal displacement illustrated, only spatial fre-

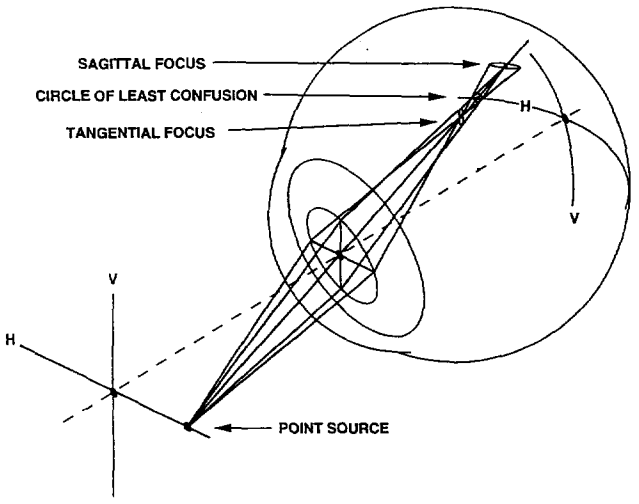

FIGURE 2. Diagram illustrating the geometry of oblique astigmatism. The dashed line corresponds to the optic axis of the eye.

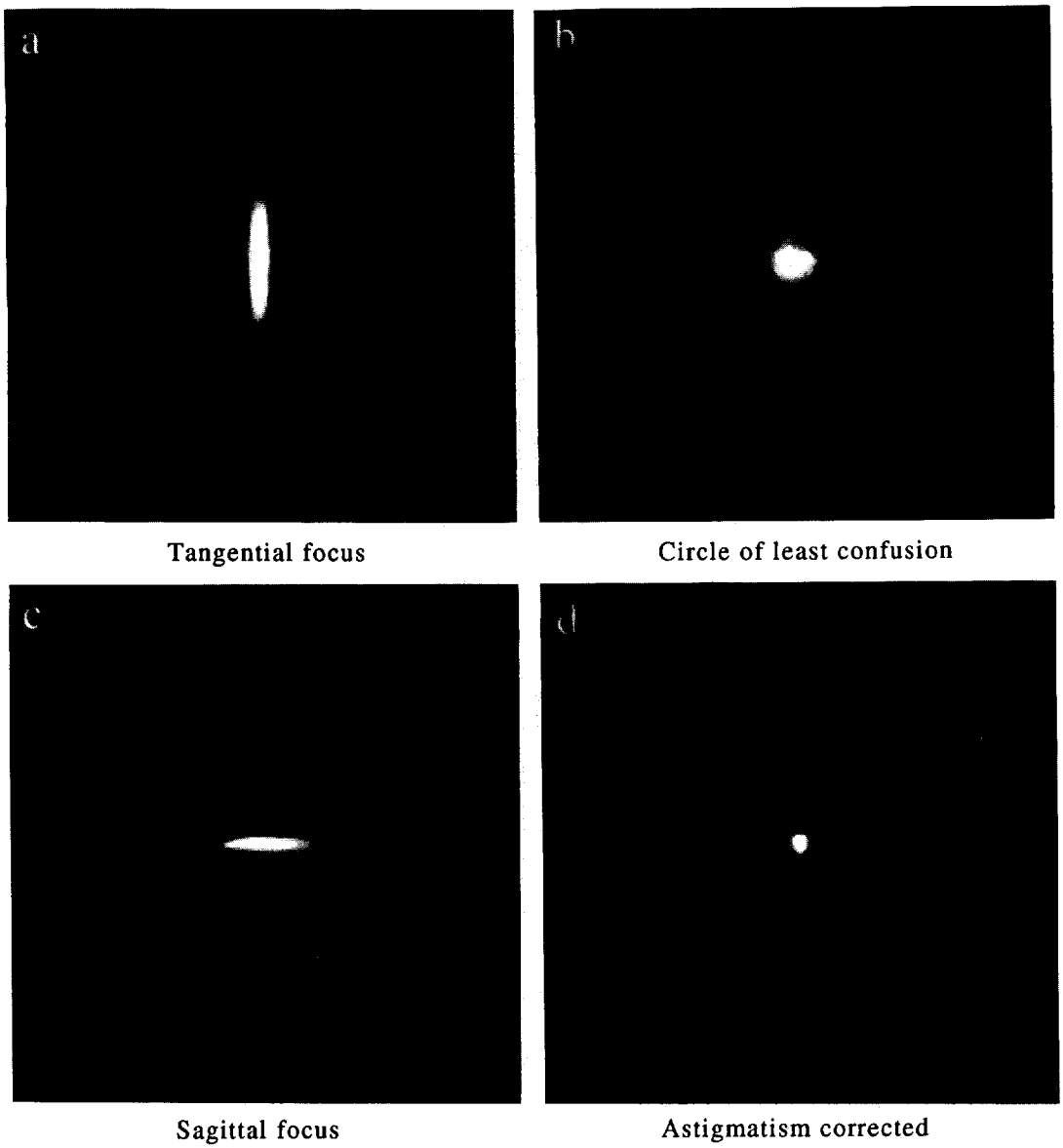

FIGURE 3. Average aerial images for subject DRW at 20 deg eccentricity in the temporal retina obtained under four different focusing conditions corresponding to (a) the tangential focus, (b) circle of least confusion, (c) sagittal focus, and (d) best focus with oblique astigmatism corrected with a cylinder lens. Each image is 2 deg on a side.

quency components corresponding to vertical gratings are in focus at the tangential focus. At the sagittal focus, the point spread function is narrowest in the direction perpendicular to the displacement of the point source and is elongated in the parallel direction. For the horizontal displacement illustrated, only spatial frequency components corresponding to horizontal gratings are in focus at the sagittal focus. The circle of least confusion occurs midway between the two foci. For an eye with zero mean-spherical-equivalent refractive error viewing an infinitely distant point source, the circle of least confusion lies on the retina, the tangential focus in front, and the sagittal focus behind. The difference in diopters between the tangential and sagittal foci is the Sturm interval.

Figure 3(a,b,c) show aerial images at the tangential focus, circle of least confusion, and sagittal focus, respectively. Each is the average of 10 images acquired at 20 deg eccentricity for observer DRW. Figure 3(d) shows the aerial image obtained when a cylindrical trial lens is used to correct oblique astigmatism. The aerial image is isotropic like that observed at the circle of least confusion, but smaller in size.

Figure 4 shows how the tangential focus, circle of least confusion, and sagittal focus change with eccentricity for each of the two observers. PA had no measurable astigmatism in the fovea or at 10 deg. However, oblique astigmatism grows to a value of 3.5 diopters at 40 deg. DRW had 1.3 diopters of against the rule astigmatism (negative cylinder axis, 108 deg) in the fovea, which grew to 6.6 diopters at 40 deg when supplemented by oblique astigmatism.

MTF RESULTS

The elongation of the aerial images at the tangential

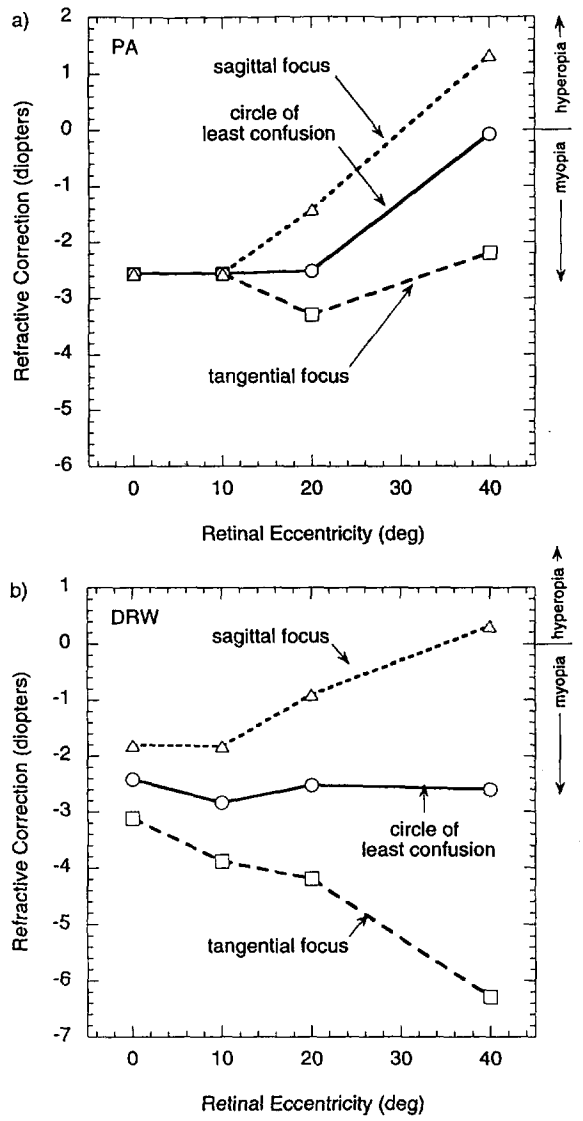

FIGURE 4. The refractive correction in diopters required to bring either the sagittal focus, the circle of least confusion, or the tangential focus into coincidence with the retina is shown as a function of retinal eccentricity in degrees. (a) Shows data for observer PA; (b) shows data for DRW.

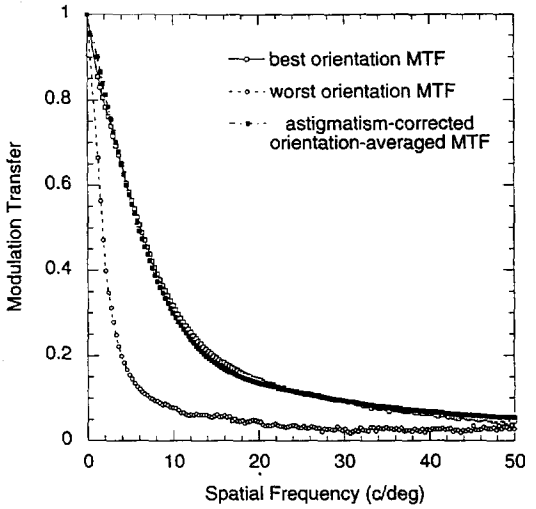

FIGURE 5. Comparison of the MTF at the best orientation with that at the worst orientation at 20 deg eccentricity. Average of two subjects, average of MTFs at the tangential and sagittal foci. Also shown is the MTF obtained by averaging across orientation when oblique astigmatism is corrected with a cylinder lens.

and sagittal foci implies that the corresponding two-dimensional MTFs will also be strongly anisotropic. Figure 5 illustrates this with one-dimensional MTFs obtained at 20 deg eccentricity. Unless explicitly stated otherwise, this and later MTF plots show the mean data for the two observers. The best orientation MTF (open squares) is the average of the MTFs at the best orientation for the tangential and sagittal foci. These orientations correspond to those of vertical gratings for the tangential focus and to those of horizontal gratings for the sagittal focus. The MTFs obtained at the tangential and sagittal foci were essentially the same except that one was rotated 90 deg with respect to the other, so we have combined these results in Fig. 5 as well as other later figures. The worst orientation MTF (open circles) is the average of the MTFs obtained 90 deg from the best orientation for the sagittal and tangential foci. The MTF corresponding to the circle of least confusion (not shown) would lie in between these two extremes. This shows that oblique astigmatism can have a large effect on retinal image quality.

If oblique astigmatism is corrected, the MTF, shown by solid squares in Fig. 5, is virtually identical to the best orientation MTF. The astigmatism-corrected MTF was computed by averaging across all orientations the isotropic two-dimensional MTF obtained when the appropriate cylindrical lens was used to correct oblique astigmatism. This shows that the anisotropy in the aerial image at the tangential and sagittal foci is due to oblique astigmatism, since it can be removed with a suitable cylindrical correction.

Figure 6 shows how the monochromatic MTF depends on retinal eccentricity. Figure 6(a) shows MTFs obtained when only defocus is corrected, but not oblique astigmatism. The MTF at each eccentricity is computed from the aerial images obtained when focused at the circle of least confusion. In addition to representing the average of the two observers, each MTF is averaged across all possible orientations. We will refer to these MTFs as orientation-averaged MTFs. Figure 6(b) shows estimates of the optical quality of the eye when both defocus and astigmatism are corrected. The MTFs represent the average of the best orientation MTFs at the tangential and sagittal foci. One could achieve the same result with MTFs obtained with cylindrical correction at each retinal location. However, with our real-time focusing method, we could locate the tangential and sagittal foci with greater ease and accuracy than we could typically correct astigmatism with discrete trial lenses.

The data of Fig. 6(a,b) have been least squares fit with the sum of two exponentials (Navarro *et al.*, 1993),

$$M(s) = (1 - c)e^{-as} + ce^{-bs} \quad (1)$$

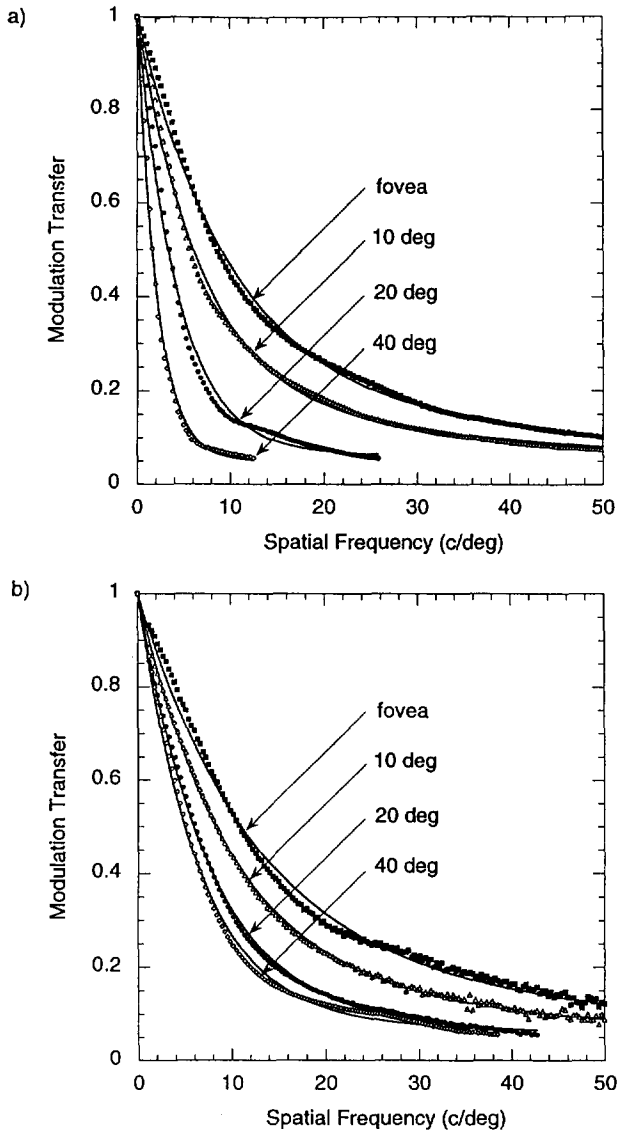

FIGURE 6. (a) MTFs at eccentricities of 0, 10, 20 and 40 deg (open diamonds) in the horizontal meridian of the temporal retina computed from aerial images obtained at the circle of least confusion, without correction for oblique astigmatism. The data are averaged across all orientations and both observers. These MTFs provide an estimate of the average optical quality of the eye when off-axis refractive errors have been corrected but oblique astigmatism has not. All curves have been least squares fit with the sum of two exponentials. (b) MTFs at the same eccentricities computed from aerial images obtained at the tangential and sagittal foci. The MTFs at the orientations in each case that produced the best image quality were averaged. Average of two subjects. These MTFs provide an estimate of the optimum image quality that can be obtained across the retina when both defocus and astigmatism are corrected.

where $M(s)$ is the modulation transfer and s is spatial frequency. This function provides a fair fit to the data, though the data often show a subtle shoulder at intermediate spatial frequencies that is not captured by it. Table 1 lists the coefficients, a, b and c for the fits. Computed values of the MTF below 0.05 tend to become unreliable, so we restricted the fits to values above 0.05. The fits depart quickly from the data at contrasts lower than about 5%.

TABLE 1. Coefficients for least squares fit of the sum of exponentials to MTF data

	Circle of least confusion			Astigmatism corrected		
Ecc.	*a*	*b*	*c*	*a*	*b*	*c*
Fovea	0.0122	0.0988	0.8172	0.0129	0.0816	0.7921
10 deg	0.0154	0.1466	0.8266	0.0140	0.1036	0.8299
20 deg	0.0000	0.2305	0.9378	0.0082	0.1313	0.9120
40 deg	0.0000	0.4663	0.9515	0.0059	0.1555	0.9178

Fits are to average data of the two observers. "Circle of least confusion" refers to the data of Fig. 6(a), which are orientation-averaged MTFs obtained without correcting oblique astigmatism and with a refractive state corresponding to the circle of least confusion. "Astigmatism-corrected" refers to the data of Fig. 6(b), which are the MTFs obtained when defocus and oblique astigmatism have been corrected.

We found that the orientation-averaged MTFs computed at each end of the Sturm interval were essentially identical to that corresponding to the circle of least confusion. So although the MTF exhibits a strong orientation dependence across the Sturm interval, the optical quality averaged across orientation hardly changes at all. Therefore, the orientation-averaged MTFs shown in Fig. 6(a) serve as a rough guide to the average optical quality that might be encountered for objects over a relatively wide range of object distances.

The curves in Fig. 6(b) put an upper bound on the optical quality of the eye in the peripheral retina because they were obtained under conditions in which both defocus and oblique astigmatism were corrected. Further improvements in image quality at this pupil size could only be obtained by correcting higher-order aberrations. These data estimate the retinal contrast that can be obtained with monochromatic one-dimensional stimuli such as gratings that are optimally focused. They also represent the performance for two-dimensional stimuli when the appropriate cylindrical correction is applied to correct astigmatism. The reduction in the quality of images of the peripheral fundus is reduced by off-axis aberrations (Wang *et al.*, 1983). The data of Fig. 6 provide quantitative estimates of this reduction.

DISCUSSION

The MTFs reported here are consistently higher than those reported by Navarro *et al.* (1993). This is not due to individual differences because it was true for PA, who was an observer for both studies. Figure 7 shows individual results for PA at the fovea (circles) and at 40 deg (squares). Solid symbols show data from the present study and are the orientation-averaged MTFs obtained with the refractive state corresponding to the circle of least confusion. (Because PA has no astigmatism at the fovea, this corresponded to the best focus possible.) Open symbols show the data from the study of Navarro *et al.* Oblique astigmatism was not corrected in either data set shown in Fig. 7. In the study of Navarro *et al.*, the refractive state at 40 deg was near the tangential focus

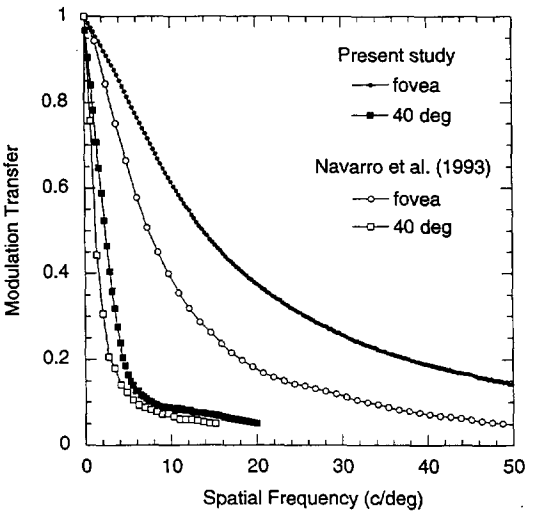

FIGURE 7. Comparison of the MTFs at the fovea and at 40 deg for the single observer, PA, who participated in the study of Navarro *et al.* as well as the present study. The data from the present study were collected with the eye refracted on the circle of least confusion, without correction for oblique astigmatism at 40 deg. At the fovea, this observer showed no astigmatism of any kind.

instead of the circle of least confusion. We do not think this explains the difference because we consistently found that the orientation-averaged MTF is independent of refractive state across the entire Sturm interval. That is, though the orientation that is in best focus shifts from horizontal to vertical across this range, the MTF averaged across all orientations is unchanged.

There are several possible reasons for the difference between the two studies. First, Navarro *et al.* used a 4 mm pupil whereas the present study used 3 mm, which gives a somewhat higher MTF (Campbell & Gubisch, 1966). For any dioptric amount of oblique astigmatism, the blur circle on the retina scales with pupil diameter, so the smaller pupil used in the present study would be expected to produce a higher MTF. Second, the present study used 543 nm light, which produces a slightly higher MTF than the 632.8 nm light used by Navarro *et al.* (Williams *et al.*, 1994). Also, Navarro *et al.* used near viewing with free accommodation which could produce a significant lag in accommodation. The present study used paralyzed accommodation and distant viewing. Navarro *et al.* explicitly chose experimental conditions that would mimic normal viewing conditions outside the laboratory whereas the present study chose conditions to optimize optical quality.

Oblique astigmatism and peripheral refractive error

The changes in the refractive error and oblique astigmatism with retinal eccentricity shown in Fig. 4 are consistent with earlier studies (reviewed by Charman, 1983). The relatively large apparent amount of oblique astigmatism for DRW at large eccentricities (6.8 diopters at 40 deg) is probably augmented by the astigmatism of the same sign observed near the optic axis. There is a rather rich diversity in the pattern across individuals (Ferree *et al.*, 1931; Ferree & Rand, 1933; Rempt *et al.*, 1971), and the differences between the two observers in this study are therefore not surprising. We also found a substantial difference between the MTFs of our two observers, with PA having better retinal image quality than DRW at all eccentricities, even when defocus and astigmatism were corrected. This is consistent with earlier reports of large individual differences in foveal MTFs computed from wave aberration measurements (Walsh *et al.*, 1984).

The comparison of Fig. 6(a,b) provides an assessment of the effect on modulation transfer of oblique astigmatism; at large eccentricities particularly, the corresponding curves drop much more rapidly in the case where astigmatism is uncorrected. Nonetheless, there is a decline in image quality even when oblique astigmatism is corrected, indicating that it is not the only cause of the deterioration of optical quality with retinal eccentricity. Other aberrations, such as coma, must also grow with increasing eccentricity. It is difficult to identify these specific aberrations with the double pass procedure because phase information is lost (Artal *et al.*, 1995). Artal *et al.*, (1996) and Navarro and Losada (1996) have introduced a variant of the double pass procedure that allows recovery of the phase information so that the wave aberration can be estimated. Direct measurements with wavefront sensing techniques could also be used to identify these off-axis aberrations (Walsh *et al.*, 1984; Liang *et al.*, 1994).

Off-axis optical quality and retinal sampling

A large number of studies have suggested that the optics of the eye have little or no influence on peripheral visual acuity, implying that neural factors pose the fundamental limit. Comparisons of acuity for interference fringes and conventional gratings in peripheral retina have either found no difference (Green, 1970; Thibos *et al.*, 1987a) or a relatively small one (Frisén & Glansholm, 1975). Studies that have examined the effect of refractive state on visual acuity for conventional acuity targets usually have shown no effect, at least for modest changes in refractive state (Millodot *et al.*, 1975; Rempt *et al.*, 1976; Rovamo *et al.*, 1982). On the other hand, the refractive state of the peripheral retina apparently does influence other measures of visual performance, such as detection threshold (Fankhauser & Enoch, 1962) and motion threshold (Johnson & Leibowitz, 1974).

Here we address the question of the effect of optical blur on the visibility of aliasing in peripheral retina. In and near the fovea, the spatial sampling rate of photoreceptors and subsequent neural arrays is high compared to the optical quality of the eye. This has led to the view that the optics play a protective role in the fovea (Snyder & Miller, 1977). Observing aliasing there usually requires the use of interference fringe stimuli (Byram, 1944; Campbell & Green, 1965; Williams, 1985b, 1988, 1992), though chromatic aliasing, attributable to sampling effects of submosaics of cones, can sometimes be seen with conventional gratings (Williams

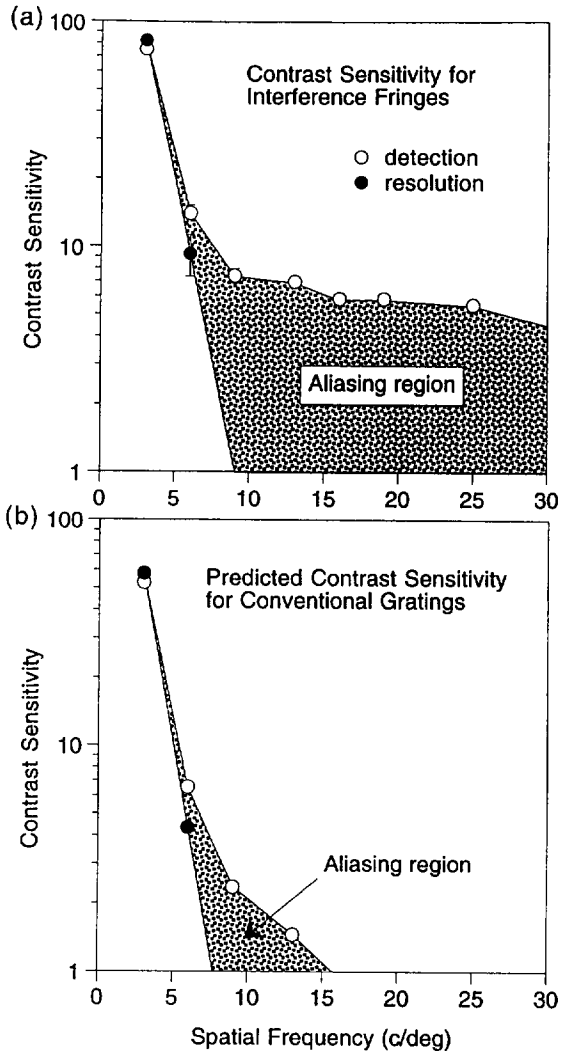

FIGURE 8. (a) Forced-choice contrast sensitivity for interference fringes at an eccentricity of 20 deg in the horizontal meridian of the temporal retina for observer DRW. The data have been slid upward by a factor of 4 to compensate for masking by laser speckle. Open circles show contrast sensitivity for detecting which of two intervals contained the fringe; solid symbols show contrast sensitivity for identifying the fringe orientation. The stippled region indicates the region in which aliasing occurs. (b) Same as (a) except that the data have been multiplied by the MTF of the eye for this observer at this eccentricity. The MTF used was that obtained when both defocus and oblique astigmatism were corrected. Note the large reduction in the aliasing region caused by optical blurring despite the modest change in the predicted fringe resolution.

et al., 1991). The rapid decline in neural sampling rates and the relatively slow decline in optical quality leads to the expectation that the peripheral retina should be particularly susceptible to aliasing effects (Yellott, 1982). Indeed, aliasing has been observed in peripheral retina with interference fringes (Coletta & Williams, 1987; Thibos *et al.*, 1987a,b; Williams & Coletta, 1987; Coletta *et al.*, 1990; Galvin & Williams, 1992), and it is also visible there with conventional, incoherent gratings (Smith & Cass, 1987; Anderson & Hess, 1990; Galvin & Williams, 1992; Artal *et al.*, 1995). In addition, it is clear that aliasing in the peripheral retina involves undersampling by a post-receptoral array or arrays as well as the cone mosaic (Smith & Cass, 1987; Thibos *et al.*, 1987a,b; Anderson & Hess, 1990; Galvin *et al.*, 1996).

Our new estimates of the off-axis MTF allow a more quantitative examination of the role the optics play in reducing aliasing in peripheral vision. Figure 8 shows that the effect of optical blurring at 20 deg can be substantial on aliasing, without much affecting visual acuity. Figure 8(a) shows contrast sensitivity obtained with interference fringes at an eccentricity of 20 deg in the temporal retina for observer DRW. Open symbols show contrast sensitivity for detection, i.e., identifying the interval containing the grating. Solid symbols show contrast sensitivity for resolution, i.e., identifying the orientation of the grating. The raw contrast sensitivity data for both detection and resolution have been shifted upward by a factor of 4 to take account of the contrast sensitivity reduction for laser interference fringes caused by laser speckle (Williams, 1985b). This estimate of speckle masking was obtained for this same observer in the same range of spatial frequencies, but in the fovea. We assume here that it would be similar in peripheral retina, but in any case the exact value is not important for our argument.

At the lowest spatial frequency where the fringe can be easily resolved, contrast, sensitivity for detection and resolution agree. However, with increasing spatial frequency, contrast sensitivity for resolution plummets. Linear extrapolation on the semilog plot predicts an acuity of about 9 c/deg. However, contrast sensitivity for detection has a broad shallow shoulder extending beyond 25 c/deg, revealing a large aliasing region, shown stippled in the figure.

Figure 8(b) shows the same contrast sensitivity data multiplied by the modulation transfer function of this observer's optics when oblique astigmatism is corrected. Note that visual acuity hardly changes at all when optical blurring is introduced, consistent with the reports in the literature cited above. Indeed, we suspect that our crude extrapolation overestimates the change in acuity; unpublished measurements of foveal resolution as a function of contrast indicate an even steeper slope than shown, which would reduce still further the small effect of the optics on acuity. Indeed, Thibos *et al.* (1996) made measurements of the resolution limit for conventional gratings as a function of contrast at 30 deg eccentricity. They found that the slope was infinite for contrasts above about 20%, which would make the resolution limit completely invariant over a five-fold range of contrasts from 20 to 100%. Despite the relative invulnerability of resolution, the aliasing region has been drastically reduced. The range of spatial frequencies over which aliasing can be seen now extends only to about 16 c/deg, which agrees well with an estimate of 15 c/deg made with conventional gratings at this retinal location for this observer with defocus and astigmatism corrected (Galvin & Williams, 1992). This shows that even optics corrected for defocus and astigmatism can produce a large reduction in aliasing, without much affecting acuity. The aliasing,

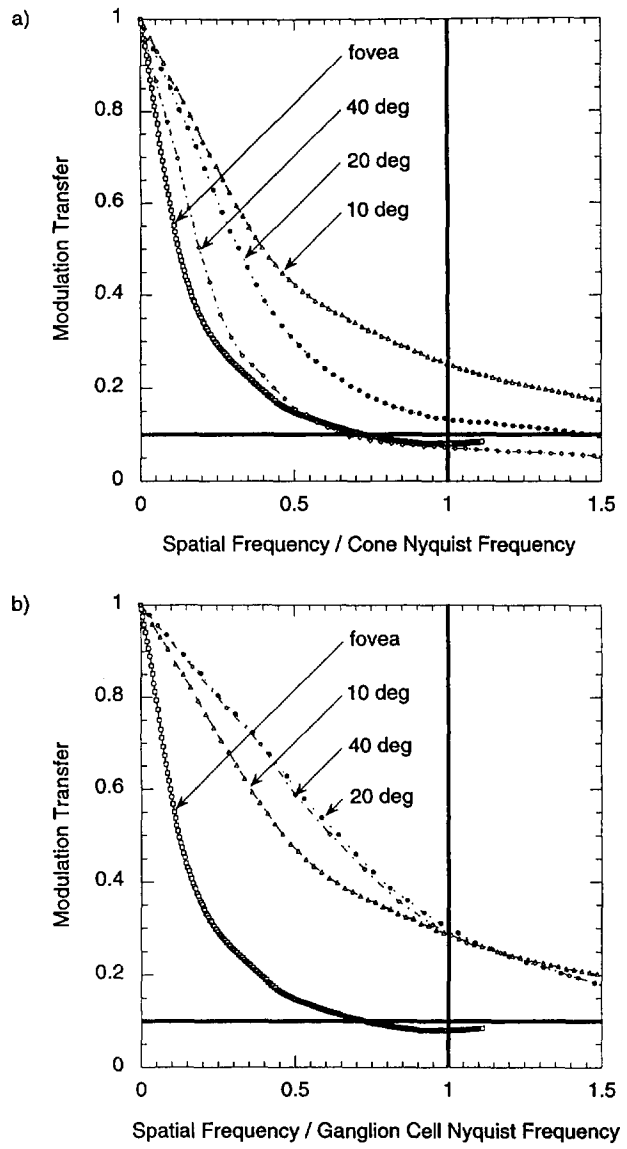

FIGURE 9. (a) The data of Fig. 6(a) with the spatial frequency axis normalized by the cone Nyquist frequency at each retinal eccentricity. This figure estimates the susceptibility to cone aliasing when defocus has been corrected but oblique astigmatism remains. The vertical line at a value of 1 indicates the Nyquist frequency. The horizontal line at a modulation transfer of 0.1 provides a conservative estimate of the retinal modulation below which there is no chance of observing aliasing. The region below each MTF, above the Nyquist frequency, and above the horizontal line indicates conditions in which aliasing could occur. The size of this region is a measure of the visual system's susceptibility to cone aliasing with grating stimuli. (b) Same as (a) showing the data of Fig. 6(a) with the spatial frequency axis normalized by the Nyquist frequency of the total ganglion cell population at that eccentricity. This figure illustrates the susceptibility to ganglion cell aliasing at various retinal eccentricities when defocus has been corrected but oblique astigmatism remains.

protection afforded by the optics would be even larger when defocus and oblique astigmatism have not been corrected, as is the typical case in normal viewing.

Figures 9 and 10 estimate the protection against aliasing provided by the optics at each eccentricity. We consider the potential for aliasing at either of two stages in the retina, the cone mosaic or the array of ganglion cells. Figure 9 shows the protection afforded by the optics when no correction has been made for oblique astigmatism. Figure 9(a) shows the orientation-averaged MTFs from Fig. 6(a) replotted on an abscissa in which spatial frequency has been normalized by the cone Nyquist frequency at that eccentricity. The Nyquist frequency, indicated by the vertical line, corresponds to the spacing between rows of human cones in a triangularly packed mosaic with the cone densities measured by Curcio *et al.* (1990) in the temporal retina. The cone Nyquist frequencies at 0, 10, 20 and 40 deg were 69.2, 14.0, 10.8 and 8.7 c/deg, respectively.

In our experience, nowhere in the retina can aliasing effects be seen with gratings having retinal contrasts much less than about 10% and usually they require much

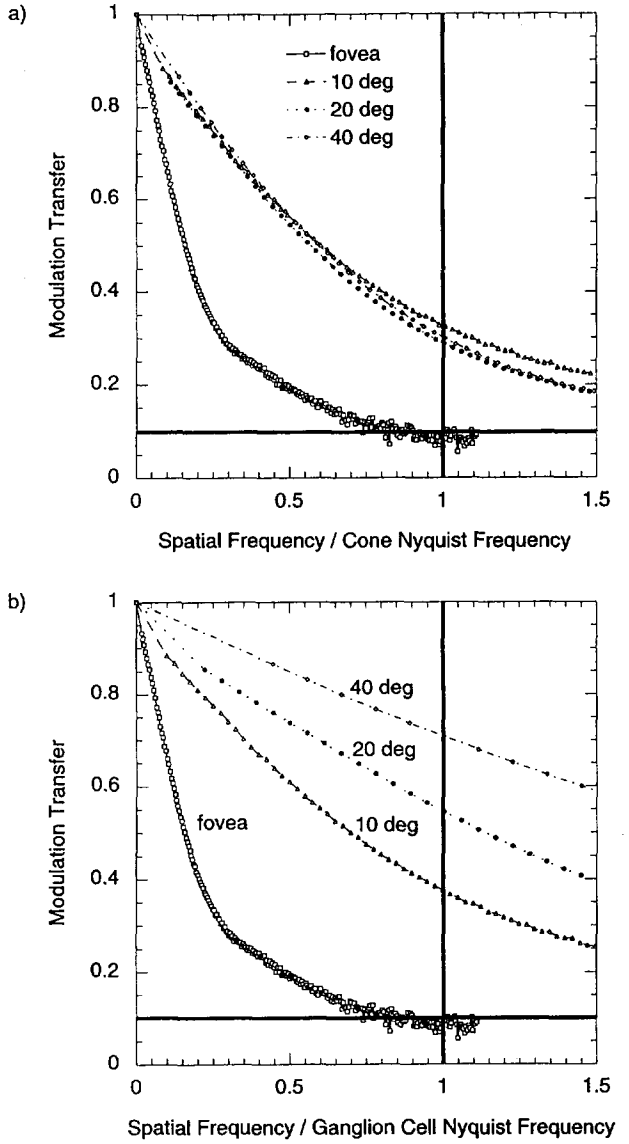

FIGURE 10. (a) Same as Fig. 9(a), except using the data of Fig. 6(b). This figure estimates the susceptibility to cone aliasing when the off-axis optical quality of the eye has been optimized, i.e., both defocus and oblique astigmatism have been corrected. (b) Same as Fig. 9(b), except using the data of Fig. 6(b). This figure estimates the susceptibility to ganglion cell aliasing when the off-axis optical quality of the eye has been optimized, i.e., both defocus and oblique astigmatism have been corrected.

higher contrasts than this. Blurring by the apertures of individual cones plays only a small role but neural factors, perhaps associated with disorder in the relevant sampling arrays (Yellott, 1982, 1983), limit the contrast sensitivity for aliasing substantially even when the optics cannot play a role. We expect that the optics will preclude aliasing of gratings when the MTF drops below a value of 10%, shown as a horizontal line in the figure. In this plot then, the visual system may be susceptible to cone aliasing only in the enclosed region below the MTF, above the horizontal line, and at spatial frequencies above the Nyquist frequency. In fact, this analysis overestimates the susceptibility to aliasing because neural losses in contrast sensitivity increase with spatial frequency rather than staying constant. But a more refined analysis will require measurements of interferometric contrast sensitivity for aliasing at a number of eccentricities. The data show that the greatest susceptibility to cone aliasing occurs in an annular region at intermediate eccentricities around 10 deg. In the fovea, the cone Nyquist frequency is sufficiently high to protect it. At 40 deg, the growth of oblique astigmatism blurs the retinal image enough to protect against aliasing despite the coarse spacing between cones there.

Figure 9(b) shows the same analysis for ganglion cells. We consider the total ganglion cell population and do not distinguish here between the various classes of ganglion cell. If one were to consider a subpopulation of cells such as the midget system, or were to consider a pair of on- and off-center cells as a single spatial sample, the analysis would not change qualitatively, although the susceptibility to aliasing would increase slightly. The Nyquist frequency corresponds to the spacing between rows of human ganglion cells in a triangularly packed mosaic with the densities measured by Curcio and Allen (1990) in the temporal retina. The ganglion cell Nyquist frequencies at 0, 10, 20 and 40 deg were 69.2, 12.1, 5.4 and 2.7 c/deg, respectively. At the fovea, we used a Nyquist frequency corresponding to that of the cones, because the sampling rate is limited by that stage rather than by ganglion cells. Compared to the cone analysis, the susceptibility to aliasing is greater overall. Outside the fovea, the MTFs lie quite near each other, indicating that the susceptibility to aliasing remains roughly constant.

The pattern of susceptibility to aliasing is different when oblique astigmatism is corrected. This analysis is particularly relevant to experimental situations in which oblique astigmatism can be corrected in the laboratory. It also shows the susceptibility to aliasing for object spatial frequencies in normal viewing at the appropriate orientation and distance to be focused on the retina, despite the presence of oblique astigmatism. Not surprisingly, outside the fovea the susceptibility to aliasing is considerably higher. Figure 10(a) shows that for cones, the fovea is well protected from aliasing as before, but all peripheral locations have greater and roughly equal susceptibility. For ganglion cells, shown in Fig. 10(b), aliasing susceptibility increases dramatically and monotonically with retinal eccentricity. With astigmatism corrected, the protection afforded by the optics at 40 deg, for example, is modest with the MTF dropping only as far as to 70% at the Nyquist frequency. The far periphery is clearly the place to look for post-receptoral aliasing, as long as care is taken to correct oblique astigmatism. Perhaps the ganglion cells can afford the modest optical protection there, since the large center sizes of ganglion cell receptive fields in the periphery offer additional protection against post-receptoral aliasing.

Additional factors mediate against aliasing in normal viewing conditions outside the laboratory. Thibos (1987) has shown that lateral chromatic aberration severely degrades image quality in the peripheral retina when polychromatic light is used. The degradation is most severe for spatial frequencies that are perpendicular to the retinal meridian because the retinal images formed at different wavelengths are displaced radially by their magnification differences. In the horizontal meridian, for example, vertical spatial frequencies are strongly blurred but horizontal spatial frequencies are not. For white light gratings, whether interferometric or not, the most visible aliasing effects should be found with gratings oriented parallel to the retinal meridian in which they lie. Another important factor is that contrast decreases with increasing spatial frequency for natural stimuli (Field, 1987). In a study to examine this factor, Galvin and Williams (1992) showed that even when the peripheral retina was carefully refracted, aliasing could not be seen with high contrast edge stimuli, which, unlike gratings, are a common stimulus in the natural environment.

Snyder *et al.* (1986) theorized that the optical quality of the eye should be significantly superior to the potential resolution of the cone mosaic across the retina. They argued that in the optimum eye design the MTF would extend beyond the cone Nyquist frequency because it increases contrast sensitivity at subNyquist frequencies, while incurring only a modest cost of susceptibility to aliasing. The present study, like earlier studies of image quality across the retina, clearly supports the view that the optics are superior to the sampling limitations of the human retina. That human cones can be imaged in the intact eye even when they lie near the foveal center further substantiates this view (Miller *et al.*, 1996). But even with the optical MTF extending above both the receptoral and postreceptoral Nyquist frequencies, the blurring the optics do impose the nature of the visual environment, and the limits of neural sensitivity conspire to prevent aliasing from disrupting normal vision in all but occasional viewing conditions, not only at fixation but throughout the visual field.

REFERENCES

Anderson, S. J. & Hess, R. F. (1990). Post-receptoral undersampling in normal human peripheral vision. *Vision Research, 30*, 1507–1515.

Arnulf, A., Santamaria, J. & Bescos, J. (1981). A cinematographic method for the dynamic study of the image formation by the human eye. Microfluctuations of the accommodation. *Journal of Optics, 12*, 123–128.

Artal, P., Derrington, A. M. & Colombo, E. (1995). Refraction, aliasing, and the absence of motion reversals in peripheral vision. *Vision Research, 35*, 939–947.

Artal, P., Iglesias, I., Lopéz-Gil, N. & Green, D. G. (1995). Double-pass measurements of the retinal-image quality with unequal entrance and exit pupil sizes and the reversibility of the eye's optical system. *Journal of the Optical Society of America A, 12*, 2358–2366.

Artal, P., Marcos, S., Navarro, R. & Williams, D. R. (1995). Odd aberrations and double pass measurements of retinal image quality. *Journal of the Optical Society of America A, 12*, 195–202.

Byram, G. M. (1944). The physical and photochemical basis of visual resolving power. Part II. Visual acuity and the photochemistry of the retina. *Journal of the Optical Society of America, 34*, 718–738.

Campbell, F. W. & Green, D. G. (1965). Optical and retinal factors affecting visual resolution. *Journal of Physiology (London), 181*, 576–593.

Campbell, F. W. & Gubisch, R. W. (1966). Optical quality of the human eye. *Journal of Physiology (London), 186*, 558–578.

Charman, W. N. (1983). The retinal image in the human eye. In: Osborne, N. & Chader, D. (Eds), *Progress in retinal research*, vol. 2, (pp. 1–50). Oxford: Pergammon Press.

Charman, W. N. & Jennings, J. A. M. (1976). The optical quality of the monochromatic retinal image as a function of focus. *British Journal of Physiology and Optics, 31*, 119–134.

Coletta, N. J. & Williams, D. R. (1987). Psychophysical estimate of extrafoveal cone spacing. *Journal of the Optical Society of America, 4*, 1503–1513.

Coletta, N. J., Williams, D. R. & Tiana, C. L. M. (1990). Consequences of spatial sampling for human motion perception. *Vision Research, 30*, 1631–1648.

Curcio, C. A. & Allen, K. A. (1990). Topography of ganglion cells in human retina. *Journal of Comparative Neurology, 300*, 5–25.

Curcio, C. A., Sloan, K. R., Kalina, R. E. & Hendrickson, A. E. (1990). Human photoreceptor topography. *Journal of Comparative Neurology, 292*, 497–523.

Fankhauser, F. & Enoch, J. M. (1962). The effects of blur on perimetric thresholds. *Archives of Ophthalmology New York, 68*, 240–251.

Ferree, C. E. & Rand, G. (1933). Interpretation of refractive conditions in the peripheral field of vision. *Archives of Ophthalmology (Chicago), 9*, 925–938.

Ferree, C. E., Rand, G. & Hardy, C. (1931). Refraction for the peripheral field of vision. *Archives of Ophthalmology (Chicago), 5*, 717–731.

Field, D. J. (1987). Relations between the statistics of natural images and the response properties of cortical cells. *Journal of the Optical Society of America, 4*, 2379–2394.

Flamant, F. (1955). Etude de la repartition de lumiere dans l'image retinienne d'une fente. *Review Optics (theory and instrumentation), 34*, 433–459.

Frisén, L. & Glansholm, A. (1975). Optical and neural resolution in peripheral vision. *Investigative Ophthalmology, 14*, 528–536.

Galvin, S. J. & Williams, D. R. (1992). No aliasing at edges in normal viewing. *Vision Research, 32*, 2251–2259.

Galvin, S. J., Williams, D. R. & Coletta, N. J. (1996). The spatial grain of motion perception in human peripheral vision. *Vision Research*, in press.

Green, D. G. (1970). Regional variations in the visual acuity for interference fringes on the retina. *Journal of Physiology (London), 207*, 351–356.

Jennings, J. A. M. & Charman, W. N. (1978). Optical image quality in the peripheral retina. *American Journal of Optomology, Physiology Optics, 55*, 582–590.

Jennings, J. A. M. & Charman, W. N. (1981). Off-axis image quality in the human eye. *Vision Research, 21*, 445–455.

Johnson, C. A. & Leibowitz, H. W. (1974). Practice, refractive error, and feedback as factors influencing peripheral motion thresholds. *Perception & Psychophysics, 15*, 276–280.

Liang, J., Grimm, B., Goelz, S. & Bille, J. (1994). Objective measurement of the wave aberrations of the human eye using a Hartmann–Shack wavefront sensor. *Journal of the Optical Society of America A, 11*, 1949–1957.

Marchywka, M. & Socker, D. G. (1992). Modulation transfer function measurement technique for small-pixel detectors. *Applied Optics, 31*, 7198–7213.

Miller, D., Williams, D. R., Morris, G. M. & Liang, J. (1996). Images of cone photoreceptors in the living human eye. *Vision Research*, in press.

Millodot, M., Johnson, C. A., Lamont, A. & Leibowitz, H. W. (1975). Effect of dioptrics on peripheral visual acuity. *Vision Research, 15*, 1357–1362.

Navarro, R., Artal, P. & Williams, D. R. (1993) Modulation transfer of the human eye as a function of retinal eccentricity. *Journal of the Optical Society of America, 10*, 201–212.

Navarro, R. & Losada, M. A. (1995). Phase transfer and point spread function of the human eye determined by a new asymmetric double-pass method. *Journal of the Optical Society of America, 12*, 2385–2392.

Rempt, F., Hoogerheide, J. & Hoogenboom, W. P. H. (1971). Peripheral retinoscopy and the skiagram. *Ophthalmologica, 162*, 1–10.

Rempt, F., Hoogerheide, J. & Hoogenboom, W. P. H. (1976). Influence of correction of peripheral static vision. *Ophthalmologica Basel, 173*, 128–135.

Rovamo, J., Virsu, V., Laurinen, P. & Hyvärinen, L. (1982). Resolution of gratings oriented along and across meridians in peripheral vision. *Investigations in Ophthalmology and Vision Science, 23*, 666–670.

Santamaria, J., Artal, P. & Bescos, J. (1987). Determination of the point-spread function of human eyes using a hybrid optical-digital method. *Journal of the Optical Society of America, 4*, 1109–1114.

Smith, R. A. & Cass, P. F. (1987). Aliasing in the parafovea with incoherent light. *Journal of the Optical Society of America, A, 4*, 1530–1534.

Snyder, A. W., Bossamaier, T. R. J. & Hughes, A. (1986). Optical image quality and the cone mosaic. *Science, 231*, 499–501.

Snyder, A. W. & Miller, W. H. (1977). Photoreceptor diameter and spacing for highest resolving power. *Journal of the Optical Society of America, 67*, 696–698.

Thibos, L. N. (1987). Calculation of the influence of lateral chromatic aberration on image quality across the visual field. *Journal of the Optical Society of America, A, 4*, 1673–1680.

Thibos, L. N., Cheney, F. E. & Walsh, D. J. (1987a). Retinal limits to the detection and resolution of gratings. *Journal of the Optical Society of America A, 4*, 1524–1527.

Thibos, L. N., Still, D. L. & Bradley, A, (1996). Characterization of spatial aliasing and contrast sensitivity in peripheral vision. *Vision Research*. **VR 1078.**

Thibos, L. N., Walsh, D. J. & Cheney, F. E. (1987b). Vision beyond the resolution limit: Aliasing in the periphery. *Vision Research, 27*, 2193–2197.

Walsh, G., Charman, W. N. & Howland, H. C. (1984). Objective technique for the determination of monochromatic aberrations of the human eye. *Journal of the Optical Society of America, 1*, 987–992.

Wang, G., Pomerantzeff, O. & Pankratov, M. M. (1983). Astigmatism of oblique incidence in the human model eye. *Vision Research, 23*, 1079–1085.

Westheimer, G. & Campbell, F. W. (1962). Light distribution in the image formed by the living human eye. *Journal of the Optical Society of America, 52*, 1040–1044.

Williams, D. R. (1985a). Aliasing in human foveal vision. *Vision Research, 25*, 195–205.

Williams, D. R. (1985b). Visibility of interference fringes near the resolution limit. *Journal of the Optical Society of America, A, 2*, 1087–1093.

Williams, D. R. (1988). Topography of the foveal cone mosaic in the living human eye. *Vision Research, 28*, 433–454.

Williams, D. R. (1992). Photoreceptor sampling and aliasing in human vision. In Moore D. T. (Ed.), *Tutorials in optics* (pp. 15–28). Washington: Optical Society of America.

Williams, D. R., Brainard, D. H., McMahon, M. J. & Navarro, R.

(1994). Double-pass and interferometric measures of the optical quality of the eye. *Journal of the Optical Society of America A, 11*, 3123–3135.

Williams, D. R. & Coletta, N. J. (1987). Cone spacing and the visual resolution limit. *Journal of the Optical Society of America, A, 4*, 1514–1523.

Williams, D. R., Sekiguchi, N., Haake, W., Brainard, D. H. & Packer, O. (1991). The cost of trichromacy for spatial vision. In Lee, B. B. & Valberg, A. (Eds), *From pigments to perception* (pp. 11–22). New York: Plenum Press.

Yellott, J. I., Jr (1982). Spectral analysis of spatial sampling by photoreceptors: Topological disorder prevents aliasing. *Vision Research, 22*, 1205–1210.

Yellott, J. I., Jr (1983). Spectral consequences of photoreceptor sampling in the rhesus monkey. *Science, 221*, 383–385.

Acknowledgements—The research was also supported by grants from the National Institutes of Health, EY01319 and EY04367, an NRSA fellowship to David Brainard, EY06278, an NSF Graduate Fellowship to Matt McMahon, and a CICYT (Spain) grant TIC91-0438 to R. Navarro. Thanks to Sue Galvin for discussion.